chapter 8 – AMPKα2 and insulin-mediated vasoreactivity in skeletal muscle

AMPKα2 activation regulates microvascular perfusion and insulin-mediated vasoreactivity in skeletal muscle through control over eNOS and endothelin-1 activity

Submitted

Michiel P de Boer
Rick I Meijer
Erik A Richter
Geerten P van Nieuw Amerongen
Pieter Sipkema
Tom J A Kokhuis
Pieter Koolwijk
Victor W M van Hinsbergh
Yvo M Smulders
Erik H Serné
Etto C Eringa

Abstract

Decreased tissue perfusion is an important risk factor for the development of insulin resistance and cardiovascular disease in the obese. Obesity-associated hypoadiponectinemia and subsequent decreased 5'AMP activated kinase (AMPK) activity, in particular of its α2 kinase subunit, have been linked to insulin resistance. It is, however, unknown whether and how AMPKα2 controls microvascular perfusion. To test whether AMPKα2 controls muscle perfusion and insulin-induced vasodilation and, if so, to investigate the mechanisms involved. In isolated muscle resistance arteries of Wistar rats, effects of AMPK activation were studied, using pressure myography. Globular adiponectin (gAdn) and 5-aminoimidazole-4-carboxamide-1-β-d-ribofuranoside (AICAR) increased AMPK activity in endothelium, enabling insulin-induced vasodilation. AMPK activation inhibited insulin-induced ERK1/2 activity, and the synergistic effects of gAdn and insulin on vascular diameter could be mimicked by inhibition of the MAPK/ERK1/2 kinase pathway. Moreover, inhibition of AMPK using compound C abolished the effect of gAdn and AICAR. In mice, genetic deletion of AMPKα2 abolished the interaction between gAdn and insulin in isolated resistance arteries. In vivo, effects of AMPKα2 on muscle perfusion were studied using contrast enhanced ultrasonography (CEU) during a hyperinsulinemic euglycemic clamp. In AMPKα2-/- mice, but not in AMPKα2+/+ mice, hyperinsulinemia decreased skeletal muscle perfusion. In AMPKα2-/- mice, phosphorylation of eNOS at Ser^{1177} in resistance arteries was less than in AMPKα2+/+ mice. AMPKα2 controls muscle perfusion during hyperinsulinemia through stimulation of eNOS phosphorylation and inhibition of ERK1/2 phosphorylation. Our findings provide a novel mechanism linking AMPKα2 to regulation of insulin sensitivity and organ perfusion.

Introduction

Obesity, physical inactivity and their cardiovascular sequelae have become a health problem of pandemic proportions (1), affecting developed and developing countries alike. Both obesity and physical inactivity are cardiometabolic risk factors, as they increase the risk of developing type 2 diabetes as well as cardiovascular disease (1). 5'AMP-activated protein kinase (AMPK) has been proposed to play a pivotal role in the mechanism underlying this increased risk. AMPK, a ubiquitously expressed sensor of cellular energy status, is a critical mediator of effects of exercise and obesity on cardiometabolic function. AMPK has been shown to regulate whole-body insulin sensitivity (2) and to control eNOS activity in cultured aortic endothelial cells (3). AMPK is a heterotrimer consisting of α, β and γ subunits, of which the α subunit carries its catalytic activity (4). Two isoforms of AMPKα have been identified, of which the AMPKα2 isoform regulates insulin sensitivity in vivo (2). AMPK can be activated by multiple stimuli, including exercise, caloric restriction, metformin, the fat-derived hormone adiponectin, and synthetic compounds such a 5-aminoimidazole-4-carboxamide-1-β-d-ribofuranoside (AICAR) (4,5). The exact mechanisms involved in AMPK control over insulin sensitivity in vivo are unclear, as AMPKα2-deficient myocytes show normal insulin sensitivity (2,6). Microvascular dysfunction, characterized by increased vascular resistance, impaired endothelium-dependent vasodilation and impairment of tissue perfusion, has been shown to contribute to regulation of insulin sensitivity (7,8,9). Microvascular dysfunction may be a common cause of cardiovascular disease and type 2 diabetes, as perfusion of muscle and adipose tissue in part regulates insulin-induced glucose uptake (10). We and others have shown that microvascular endothelium is an insulin target tissue (11,12,13) and participates in control of insulin sensitivity by regulating delivery of insulin and glucose to muscle (7). In muscle resistance arteries, insulin stimulates release of nitric oxide (NO) and endothelin (ET-1) from endothelium by activating Akt and extracellular-regulated protein kinase 1/2 (ERK1/2), respectively (14,15). In states of vascular insulin resistance, such as obesity, the balance shifts towards less vasodilation or even vasoconstriction (11,12). Interestingly, the globular form of the AMPK-agonist adiponectin, plasma-levels of which are diminished in obesity, has recently been shown to regulate insulin's effects on muscle perfusion (16). Whether AMPK has a role in this regulation, and how such a role is fulfilled, is presently unknown, but a role for AMPK in regulating insulin sensitivity in humans was recently indicated by correlations between plasma adiponectin levels, AMPK activation and insulin sensitivity (17). We hypothesize that AMPK, and more specifically, the AMPKα2 subunit, determines insulin-induced vasoreactivity in skeletal muscle through control over eNOS and endothelin-1 activity in the arteriolar wall after activation by the adipokine adiponectin.

Methods

Animals

The investigation conformed to the Guide for the Care and Use of Laboratory Animals published by the US National Institutes of Health (NIH publication No. 85 to 23, revised 1996). The local ethics committee for animal experiments approved the procedures. To study the role of AMPK in insulin-induced vasoreactivity ex-vivo and in-vivo, male C57BL/6N mice (back-crossed for >10 generations; Taconic, Ejby, Denmark) with a deletion of the AMPKα2 (AMPKα2-/-) catalytic subunit gene, together with their AMPKα2+/+ littermates, were generated as previously described (2). For ex-vivo experiments first-order resistance arteries from the gracilis muscle were isolated. Rat ex-vivo experiments were conducted on isolated resistance arteries of cremaster muscles of healthy Wistar rats (Harlan, Horst, the Netherlands), as described (15).

Cell culture

Microvascular endothelial cells (MVECs) from human foreskin were isolated, cultured, and characterized as described (14). Two hours before the 30 minute stimulation with globular adiponectin (gAdn, 1.0 µg/mL; Enzo Life

Sciences, Antwerp, Belgium), growth factor was withdrawn from MVEC cultures. Subsequently, cells were lysed and Western blots performed.

Vasoreactivity

Acute effects of insulin (Actrapid; Novo Nordisk, Bagsværd, Denmark) on the diameter of resistance arteries were studied by exposing arterial segments to 4 concentrations of insulin (0.02, 0.2, 2, and 20 nmol/L) as described (12,15). Insulin was added to the vessel bath in a stepwise fashion, starting at the lowest concentration, and diameter changes during 30 minutes after each concentration step were recorded. Because insulin concentrations measured in vivo in the rat and mouse range between 0.02 and 2 nmol/L, the first 3 concentrations are considered physiological and the final concentration pharmacological. To study vasoconstrictor effects of insulin, skeletal muscle resistance arteries were pretreated with the competitive eNOS inhibitor L-Nitro-N-Arginine (LNA, 0.1 mmol/L; Sigma, St Louis ,USA). Vasodilator effects of insulin were assessed through pretreatment with the nonselective ET-1 receptor antagonist PD142893 (3 μmol/L; Kordia, Leiden, The Netherlands), which blocks insulin's vasoconstrictor effects (14). To study the effects of AMPK stimuli on insulin-induced vasoreactivity, vessels were pre-treated with gAdn (1 μg/mL) or the AMPK agonist 5-aminoimidazole-4-carboxamide-1-β-d-ribofuranoside (AICAR) (2.0 mmol/L, Merck, Darmstadt, Germany), with or without the AMPK inhibitor Compound C (10 μmol/L; Enzo Life Sciences, Antwerp, Belgium). The gAdn concentration used for the experiments was derived from a dose-response study of gAdn effects on endothelial cells (18). At the end of each experiment the passive (maximally dilated) diameter was assessed by adding papaverine (0.1 mmol/L; Sigma Aldrich, St Louis, USA).

Western blot

To assess the effect of AMPKα2 deletion on arterial AMPK activity, phosphorylation of its downstream substrate acetyl CoA carboxylase (ACC) was determined by Western blotting in femoral arteries of AMPKα2+/+ and AMPKα2-/- mice (n=5-7). Similarly, the contribution of AMPKα2 to eNOS phosphorylation was assessed via the phosphorylation of Ser^{1177} and Ser^{633} residues on eNOS in AMPKα2+/+ and AMPKα2-/- femoral arteries. Specific antibodies against p-ACC, ACC, Ser^{1177}p-eNOS, Ser^{633}p-eNOS and eNOS were used, and were detected using specific secondary antibodies (1:1000; Dako, Glostrup, Denmark) as described (15). To evaluate effects of AMPK-stimulation on ERK1/2 activation, rat cremaster resistance arteries were divided into 4 segments (length ~1.5 mm, ~2 μg protein per segment; n=4 rats) which were exposed for 20 minutes to solvent (controls) or insulin (2 nmol/L) in the absence and presence of gAdn (1.0 μg/mL) or AICAR (2 mmol/L). Insulin-induced ERK1/2 activation was examined as described (14) in the absence and presence of gAdn. Arteriolar segments were processed as described (19) and specific primary antibodies against p-ERK1/2 and ERK1/2 (1:1000; New England Biolabs, Ipswich, USA) were used and detected as described above. To assess AMPK activity in cultured human MVECs, phosphorylation of AMPK and its substrate ACC were determined. After protein separation on gel (10 μg/lane) and Western blotting, blots were stained with antibodies against Thr^{172} phospho-AMPKα (1:1000; Cell Signaling Technology, Boston, USA), total AMPKα (1:1000, Cell Signaling Technology), Ser^{79} phospho-ACC and total ACC (all 1:1000, Cell Signaling Technology).

3D fluorescence microscopy and capillary density

Cremaster resistance arteries (n=4 rats) were divided into 2 segments that were treated with gAdn or solvent for 15 minutes, fixated with 4% paraformaldehyde in MOPS buffer, cut open longitudinally for en-face staining and fluorescence imaging of phosphorylated AMPK as described (15). Phospho-AMPK was then examined in endothelium and smooth muscle using a primary antibody against phospho-AMPK (1:100; New England Biolabs) and a fluorescein isothiocyanate–labeled secondary antibody. 4',6-diamidino-2-phenylindole (DAPI) was used as

a nuclear counter stain. Three-dimensional images of arterial segments were obtained using a ZEISS Axiovert 200 Marianas inverted digital imaging microscope workstation using Slidebook software (Slidebook version 4.1; 3I Intelligent Imaging Innovations). Capillary densities in gastrocnemius muscle from AMPKα2+/+ and AMPKα2-/- mice were analyzed by staining endothelial cells using lectin. Slices (10 µm) were obtained from snap-frozen muscle, and capillary endothelial cells were identified by immunohistochemical staining with lectin FITC (1:100, Sigma Aldrich, St Louis, USA). Capillary density was expressed as the number of capillaries per mm2 and number of capillaries per muscle fiber.

Animal surgery

Telemetry measurement of systemic arterial blood pressure

To assess whether genetic deletion of AMPKα2 affects systemic blood pressure, AMPKα2+/+ and AMPKα2-/- mice were anesthetized with isoflurane (2-2.5% v/v). After induction of anesthesia, a telemetric device (Type: TA11PA-C10, Data Science International, St. Paul, MN, USA) was inserted in a subcutaneous pocket with a pressure-sensing probe positioned in the aortic arch (via the internal carotid artery). After two weeks of recovery blood pressure was monitored for a period of 48 hours (20).

Euglycemic, hyperinsulinemic clamp and contrast enhanced ultrasonography

Mice were anesthetized with an intraperitoneal injection of a mixture of Fentanyl (0.31 mg/kg), Midazolam (6.25 mg/kg) and Acepromazine (6.25 mg/kg) and placed on a homeothermic heating pad (Panlab, Vitrolles, France), which maintained body temperature at 38°C. The right jugular vein was cannulated with polyethylene tubing (PE-10 and PE-50) and used for intravenous infusion of microbubbles, insulin and glucose. The animals were allowed 30-45 min to stabilize after surgical procedures before the start of experimental protocols.

Microvascular perfusion imaging

Contrast-Enhanced Ultrasonography (CEU) was performed to quantify microvascular perfusion, using the setup pictured in supplementary figure S1 (20). Continuous ultrasound (Sequoia 512, Siemens Medical Systems) images of the proximal adductor muscle group (adductor magnus and semimembranosus) in the hindleg were obtained. Where indicated, animals received an infusion of phosphatidylcholine/polyethylene glycol stearate-coated decafluorobutane-filled microbubbles which were manufactured at the Erasmus University in Rotterdam as described (21). Microbubbles were infused at a rate of 5 µl/min for 5 minutes. After reaching steady-state, real-time replenishment curves were registered. A one-second, high mechanical index ultrasound pulse destroyed all microbubbles in the field of view. Next, continues low mechanical index imaging visualized microbubble inflow. Corresponding video-intensity was analyzed off-line using the Image Processing toolbox in MATLAB (Mathworks, Natick, MA). To correct for large vessels and background noise, mean video-intensity during the first half second was subtracted from the signal. The derived video-intensities were then fitted to the exponential function VI = MBV(1-e-MFV(t-0.5)), where VI is the video intensity at a given time (t in seconds) after microbubble destruction, MBV is microvascular blood volume, MFV is microvascular flow velocity which represents vascular resistance and e the natural logarithm. Microvascular blood flow (MBF) is the product of MBV*MFV (22). Mean video-intensity in the region of interest was normalized for the video-intensity in a large vessel to correct for differences in systemic bubble-concentrations, generating measurements comparable within and between animals.

Euglycemic, hyperinsulinemic clamp

Insulin's effects on glucose uptake and muscle perfusion were studied using the hyperinsulinemic, euglycemic clamp technique as described (23). In short, insulin sensitivity was assessed using a primed euglycemic hyperinsulinemic clamp; 200 mU/kg; Actrapid, Novo Nordisk, France, followed by continuous insulin infusion (3

mU/kg/min) for 60 minutes, together with variable infusion of 20% D-glucose to maintain euglycemia. Blood glucose was assessed from the tail vein with a Freestyle Precision Xceed (Abbott, Hoofddorp, The Netherlands), and maintained at 5 mmol/l by adjusting the variable glucose infusion rate., Insulin sensitivity was determined by averaging the mean glucose infusion rate during the last 30 minutes.

Statistical analyses

Normally distributed data are presented as mean ± SEM. gAdn-mediated increases in pAMPK and pACC staining were tested against a normalized control of 1 by a Mann-Whitney test. Ex-vivo vasoreactivity was tested for differences with a one-way ANOVA with Bonferroni post-hoc correction. Differences between AMPKα2+/+ and AMPKα2-/- mice were tested with the unpaired t-test. Changes within mice were analyzed with a paired t-test. A two-tailed P-value of <0.05 was considered significant. All analyses were performed using the statistical software package SPSS (version 18.0, SPSS, Inc., Chicago, USA).

Results

Globular adiponectin activates AMPK in microvascular endothelium

Human microvascular endothelial cells expressed both AMPKα1 and α2, as determined by Western blot (figure 1a). Using 3D fluorescence microscopy, we found that phosphorylated AMPKα was present at the cell membrane, in the cytoplasm and in the nucleus of endothelial cells (supplemental figure S2). In these cells, exposure to gAdn increased phosphorylation of the AMPK substrate ACC (figure 1c) without increasing phosphorylation of AMPKα (figure 1b). In rat muscle resistance arteries, Thr^{172}-phosporylation of AMPKα was visible in part of the control cells in particular at the nuclei. After stimulation with gAdn, pAMPKα was redistributed showing increased phosphorylation specifically at the cell membrane and in the cytoplasm of endothelial cells, (figure 1d).

Activation of AMPK induces insulin-induced vasodilation in isolated muscle resistance arteries by stimulating NO and inhibiting ET-1 activity.

As we observed earlier, insulin exerted both vasodilator and vasoconstrictor effects on muscle resistance arteries, resulting in a neutral effect on vascular diameter under baseline conditions (figure 2a) (14,15). In contrast, after pre-treatment with either gAdn or AICAR, insulin induced a concentration-dependent vasodilation (figure 2a). The effect of gAdn on insulin-induced vasodilation was completely abolished by the AMPK inhibitor compound C (figure 3a). AICAR instead of gAdn shows similar results (data not shown). gAdn preincubation by itself did not induce changes in vessel diameter (70 ± 6.2 vs. 71 ± 6.1 µm, p=0.9). AICAR did directly induce a 20% vasodilation before the addition of insulin (19). Subsequently, we assessed whether AMPK activation changed insulin's vasodilator and/or vasoconstrictor effects. Insulin induced vasodilation during ET-1 receptor blockade, and activation of AMPK by gAdn or AICAR did not further enhance vasodilation at high-physiological insulin concentrations (2 nmol/L, figure 2b). At lower physiological concentrations (at 0.2 nmol/L, figure 2b), AICAR but not gAdn, enhanced insulin-induced vasodilation. AMPK activation by AICAR did not enhance insulin-induced Ser^{473} phosphorylation of Akt in muscle resistance arteries (supplemental figure S3). In contrast to the mild effect on insulin-induced vasodilation of rat muscle resistance arteries, AMPK activation strongly inhibited insulin's vasoconstrictor effects. Insulin induced a concentration-dependent vasoconstriction during inhibition of NO synthesis with L-NA, and gAdn and AICAR both abolished this effect (figure 2c). As insulin's vasoconstrictor effects depend on ERK1/2 (14), we assessed whether gAdn and AICAR inhibited insulin-induced phosphorylation of ERK1/2. Western blot analysis showed that the insulin-induced increase in ERK1/2 phosphorylation was indeed abolished by gAdn and AICAR (figure 2d).

Interaction between gAdn and insulin in muscle resistance arteries is mediated by AMPKα2

The AMPK inhibitor compound C provided pharmacological proof for the involvement of AMPK in the effect of gAdn on insulin-induced vasodilation in rat resistance arteries (figure 3a). To obtain genetic evidence whether AMPK, and in particular the AMPKα2 subunit controls the regulation of insulin-induced vasoreactivity by globular adiponectin, we studied the interaction between gAdn and insulin in gracilis muscle resistance arteries of AMKα2+/+ and AMPKα2-/- mice. Deletion of AMPKα2 abolished insulin-induced vasodilation in the presence of gAdn (figure 3b). In contrast to the vasoactive effects of insulin, deletion of AMPKα2 did not influence general endothelium-dependent vasodilation in response to acetylcholine (supplemental fig S4).

AMPKα2 deletion impairs muscle perfusion and insulin sensitivity but not blood pressure in vivo

AMPKα2-/- mice were insulin resistant, as shown by a reduction of glucose infusion rates by ~50 percent during the hyperinsulinemic, euglycemic clamp (6.8±0.3 vs 12.5±1.3 mg/kg/min, 6 vs 5 mice respectively, p=0.02). Body weight did not differ between the AMPKα2-/- and AMPKα2+/+ mice (27.5±1.2 vs 28.5±1.1 gram respectively, p=0.5). To assess whether AMPKα2 regulates muscle perfusion in vivo, we quantified muscle MBV, MFV and perfusion with CEU in AMPKα2+/+ and AMPKα2-/- mice before and during a hyperinsulinemic, euglycemic clamp (see for setup supplemental figure S1). Microvascular Blood Volume and MFV decreased significantly from baseline to hyperinsulinemia ($p<0.05$ and $p<0.0001$) in AMPKα2-/- mice (figure 4a and figure 4b). As a result, microvascular perfusion (the product of MBV and MFV) was significantly decreased in AMPKα2-/- mice during hyperinsulinemia ($p < 0.01$ vs. baseline, figure 4c). Moreover, perfusion was lower in AMPKα2-/- mice, both during baseline and hyperinsulinemia compared to AMPKα2+/+ mice (both $p<0.05$). Blood pressure and heart rate did not differ between the AMPKα2-/- and AMPKα2+/+ mice (supplemental figure S5). Structural capillary density, measured either by the number of capillaries per mm2 or per muscle-fiber, did not differ between AMPKα2-/- and AMPKα2+/+ mice (figure 4d). The absence of AMPKα2 did however induce a structural decrease in the maximal diameter of muscle resistance arteries (figure 4e).

AMPKα2 deletion reduces eNOS phosphorylation in vivo

Deletion of AMPKα2 significantly impaired the phosphorylation of ACC in mouse resistance arteries (figure 5a). In parallel, phosphorylation of eNOS at Ser^{1177}, but not Ser^{633}, was significantly less in these vessels of AMPKα2-/- mice than in AMPKα2+/+ mice (figure 5b and figure 5c). Finally, the degree of ACC phosphorylation showed a strong correlation with the amount of eNOS phosphorylation at Ser^{1177} (figure 5d).

Discussion

This study demonstrates for the first time that 1) AMPKα2 regulates muscle perfusion; 2) AMPKα2 regulates phosphorylation of eNOS in muscle resistance arteries; 3) gAdn is a physiological AMPKα2 agonist in muscle resistance arteries and 4) AMPK-agonists such as gAdn and AICAR exert their regulatory effects on vasoreactivity of muscle resistance arteries mainly via inhibition of the ERK1/2-ET-1 signaling pathway. Figure 6 shows a schematic overview of the main findings of this study in the context of Akt-mediated NO production and ERK1/2-mediated ET-1 release, which we described earlier (15,24).

We found that AMPKα2 controls muscle perfusion in vivo. This is in good agreement with our earlier demonstration that AICAR enhances muscle perfusion in rats (19) and with recent data from Zhao et al. showing that, AMPK-agonist gAdn stimulates muscle perfusion in rats (16). Here we have shown that this regulation is likely achieved through a shift in the NO/ET-1 balance in arteriolar endothelium.

In agreement with previous data from cultured endothelial cells (25), we have observed decreased phosphorylation of eNOS at Ser^{1177} in femoral arteries of AMPKα2-/- mice. These findings corroborate the immunohistochemistry results as reported by Xu et al. (26). In that study both AMPKα1-/- and AMPKα2-/- mice

showed decreased levels of Ser^{1177}-phosphorylated eNOS in skeletal muscle, the decrease being most pronounced in the latter strain. In contrast, our data show that genetic deletion of AMPKα2 does not affect phosphorylation of eNOS at Ser^{633}. The Ser^{633} phosphorylation site of eNOS has been described as an AMPK-target, with decreased phosphorylation in AMPKα1-/- and AMPKα2-/- iSRNA transfected HUVEC's in vitro (25). To explain this apparent difference, the Ser^{633} site of eNOS could be a target of AMPKα1 in arterial endothelium. In AMPKα2-/- mice, phosphorylation of eNOS at Ser^{1177} was decreased by 50% and showed a strong correlation with the amount of phosphorylation of the AMPK substrate ACC. Taken together, these data suggest that AMPKα2 is a strong determinant of eNOS phosphorylation and activity in arterial endothelium, and that this effect regulates muscle perfusion.

Globular adiponectin increased functional AMPK activity in incubated vascular tissue as determined by an increase in the phosphorylation of ACC. The absence of a concomitant increase in AMPK phosphorylation by gAdn suggests that AMPK can be activated via different pathways or modes than phosphorylation of the α subunit. Confocal microscopy of microvascular endothelial cells showed a redistribution of the AMPK phosphorylation pattern from nuclei to cytoplasm and cell membrane after stimulation by gAdn. This altered pattern could be a proxy for, or be the result of such an alternative mode of AMPK activation. Schisler et al. have recently demonstrated another alternative pathway for AMPK activation via C terminus of HSC70-interacting protein (CHIP), a chaperone and ubiquitin ligase. They found CHIP to act as a molecular chaperone to AMPK, able to induce conformational changes to the α subunit which stabilized and activated AMPK (27). Recently, Scott et al. have shown that the combination of small molecule drug A-769662 and AMP can activate naive AMPK allosterically and independently of upstream kinase signaling (28). Together with our data, this suggests that gAdn may also activate AMPK in microvascular endothelial cells in the absence of increased AMPKα phosphorylation.

Aside from effects on vascular tone, we have found that AMPKα2 controls structural properties of the muscle microcirculation. Deficiency of AMPKα2 in the muscle microcirculation reduces the maximal diameter of muscle resistance arteries, whereas capillary density was not different in the absence of AMPKα2. The reduced maximal diameter of muscle resistance arteries could be the result of inward remodeling due to unopposed ERK1/2 activity in the absence of AMPKα2 (29). This finding is in contrast with earlier data showing that capillary density is reduced in mice with muscle-specific over-expression of an inactive AMPKα2 mutant (30). This discrepancy might be explained by non-specific effects of the transgene, or redundant roles of AMPKα1 and AMPKα2 in regulation of basal capillary density.

Some functional differences were observed between the AMPK agonists gAdn and AICAR in our study. AICAR alone induces vasodilation, while gAdn does not (table 1, ref 19). Although both gAdn and AICAR uncover insulin-induced vasodilation by inhibiting insulin's vasoconstrictor effects at a high insulin concentration, AICAR does so even at low physiological insulin concentrations (figure 2a). This may be explained by a stronger effect of AICAR on AMPK activity or by a differential effect on AMPKα1 activity (and subsequent additional phosphorylation of eNOS at ser^{633} (26, figure 5)) by AICAR and gAdn. Finally, the modes of AMPK activation by the two stimuli are different, as AICAR enhances total AMPKα phosphorylation (31) while gAdn does not (figure 1).

Globular adiponectin proved a physiological AMPKα2 agonist in the muscle microcirculation. Previously, we have shown that adiponectin is produced locally in muscle by perivascular adipose tissue (PVAT) situated around resistance arteries in muscle (32). This could enable muscles to regulate their own microvascular blood volume through paracrine interaction between intramuscular PVAT and endothelial AMPKα2 (33).

Activated by a host of insulin-sensitizing stimuli and centrally localized in the regulation of energy metabolism, AMPK is an attractive target for enhancing insulin sensitivity. Indeed, AMPKα2-/- mice are insulin resistant (2 and present study). The mechanism involved in the insulin-sensitizing effects of AMPKα2 had not been well characterized, as deletion of AMPKα2 in myocytes does not reduce insulin sensitivity (6). Substitution by

redundant AMPKα1 activity in myocytes appears unlikely, as both functional and genetic double AMPKα1/α2 knockout animal models are not insulin-resistant (2,34,B. Viollet *personal communication*). Our results suggest that AMPKα2 regulates muscle insulin sensitivity through control over muscle perfusion. The observed decreased microvascular blood volume in muscles of AMPKα2-/- mice (figure 4), reflects a reduced endothelial surface area. In other studies, it has been demonstrated that a reduced endothelial surface area impairs the delivery of insulin and glucose to myocytes, resulting in reduced insulin-stimulated glucose uptake (7,8). This impairment of muscle perfusion has been observed in human insulin resistance (35) and can be induced by reducing NO availability (36) or increasing ET-1 levels (37). Here, we have shown that reducing AMPKα2 activity reduces MBV, NO availability and insulin sensitivity.

Although we expected to find an increase of MBV during hyperinsulinemia in AMPKα2+/+ mice, and an impairment of this effect in AMPKα2-/- mice, we observed a neutral effect of insulin on MBV in AMPKα2+/+ mice and a reduction of MBV in AMPKα2-/- mice (figure 4). While the average insulin effect in WT mice differs from the average response to insulin in man, responses in the latter are heterogeneous, and a significant portion of insulin-sensitive individuals shows no increase in MBV in response to insulin (35). With regards to the used mouse strain, the decrease of MBV in AMPKα2-/- mice in this study is in line with recent ex-vivo data from the same animal model (32). In that study, insulin caused vasoconstriction of AMPKα2-/- resistance arteries in the presence of PVAT ex-vivo, where AMPKα2+/+ resistance arteries showed a neutral response. These combined results suggest that a neutral vasoreactive response to insulin is a reproducible characteristic of the AMPKα2+/+ mouse phenotype. Indeed, work on collateral vessel density in ischaemia-reperfusion models has shown these vessel densities to vary between mouse strains (38). Although a different field of study, such results imply inter and intra species differences in vascular beds, both structural and functional. Of note, most work on insulin-mediated vascular reactivity in skeletal muscle using CEU has been done in rats (16,19,36). Notwithstanding the effect of insulin on vasoreactivity in AMPKα2+/+mice, the decrease in skeletal muscle perfusion induced by AMPKα2 deficiency in the current study is clear.

In conclusion, AMPKα2 regulates insulin sensitivity through structural and vasoregulatory effects in skeletal muscle perfusion. The concomitantly increased phosphorylation of eNOS and inhibition of ET-1 activity regulates microvascular perfusion, and thereby likely peripheral glucose uptake. Our findings expand on the mechanisms linking obesity, physical inactivity and insulin resistance.

Tables

table 1 - pretreatment vessel tones of the rat pressure myography experiments

	% diameter change	p		% diameter change	p
L-NA	-6.0 ± 2.0	<0.05	gAdn + L-NA	-9.9 ± 2.6	<0.01
PD142893	1.9 ± 1.4	0.23	gAdn + PD142893	-15.4 ± 3.7	<0.05
compound C	-6.2 ± 1.3	<0.01	gAdn + Compound C	-11.6 ± 5.4	0.16
gAdn	-0.1 ± 2.3	0.97			

Percentage change in vessel diameter after pre-treatment with listed compounds and before insulin dose-response experiments. L-NA = eNOS inhibitor; PD142893 = non-selective ET-1 receptor blocker; Compound C = AMPK inhibitor; gAdn = globular adiponectin. Data are given as mean and SEM.

Figures

figure 1

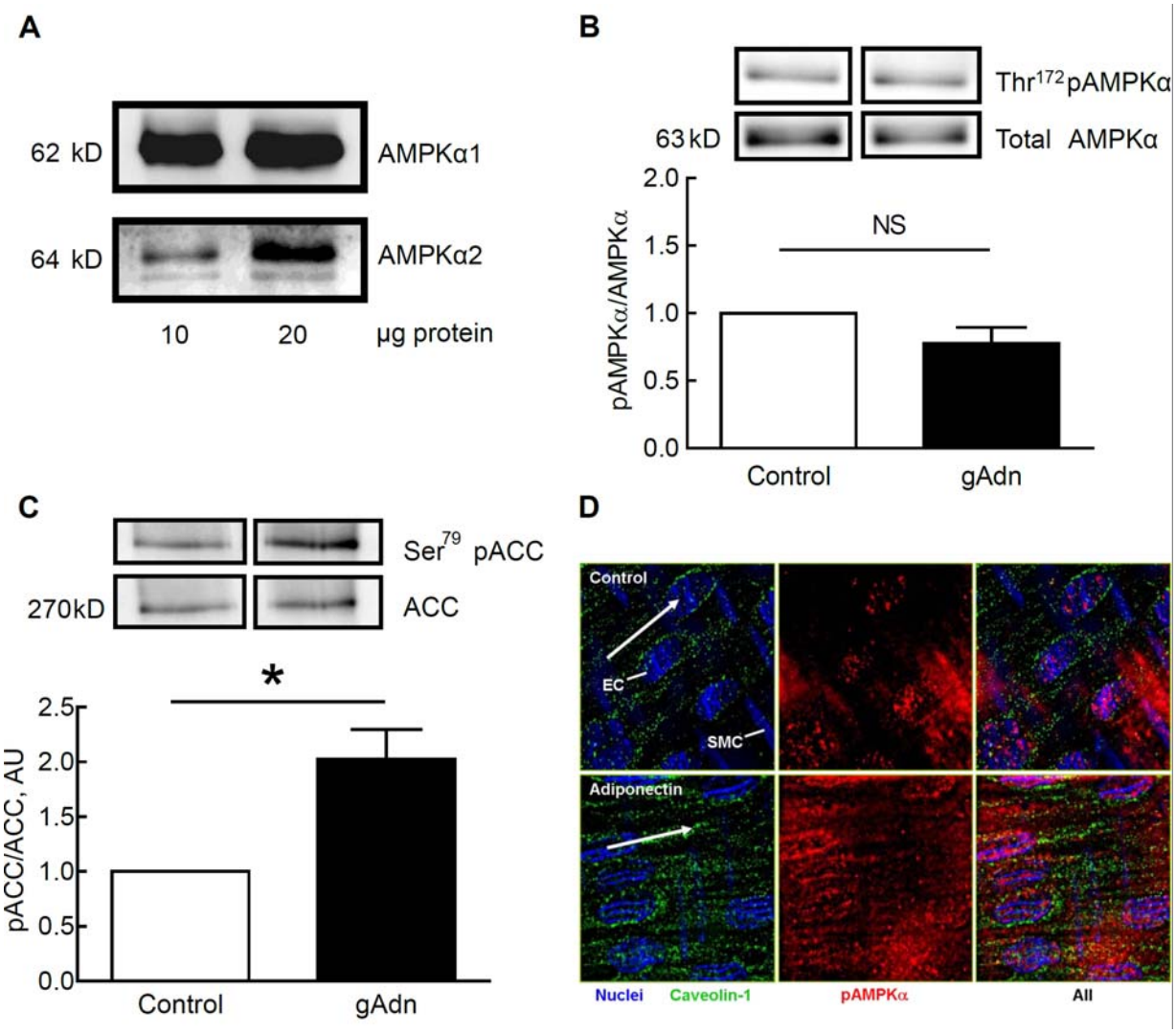

5'AMP-activated protein kinase α (AMPKα) is present in endothelial cells and is activated by globular adiponectin (gAdn). A. Both AMPKα1 and AMPKα2 are expressed in human microvascular endothelial cells (MVECs). B. gAdn does not increase overall AMPK phosphorylation at Thr^{172} in MVECs. C. Activation of AMPK by gAdn in MVECs. AMPK activity was assessed by quantification the phosphorylation of its substrate acetyl CoA carboxylase (ACC) at Ser^{79}. * $p<0.05$ gAdn vs. control. D. Activation of AMPK by gAdn and its localization in rat muscle resistance arteries. Localization of pAMPKα in endothelium of muscle resistance arteries using three-dimensional deconvolution microscopy at 63x magnification. Arrow indicates the direction of blood flow. SMC=smooth muscle cell, EC=endothelial cell.

figure 2

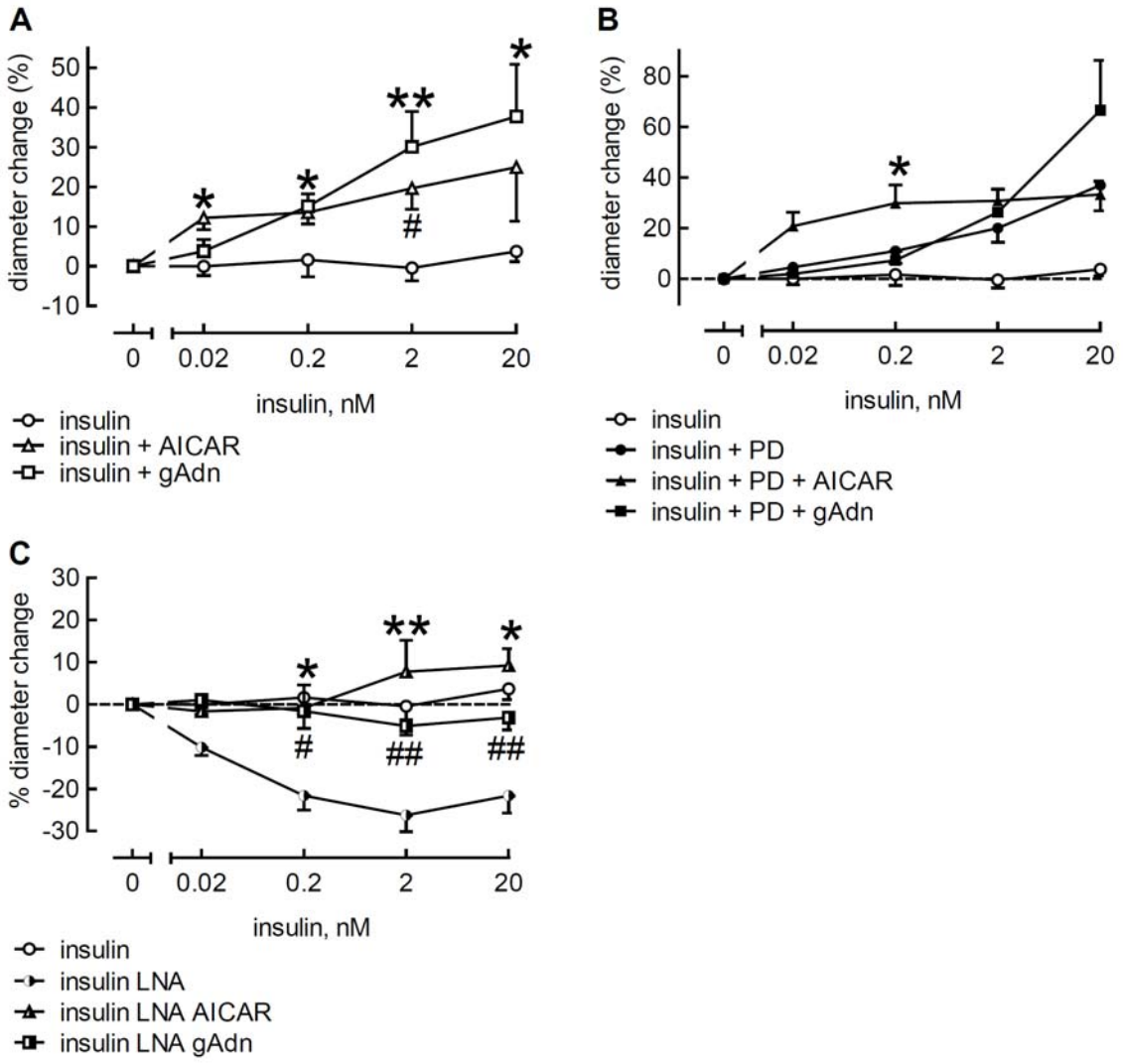

Vasoreactivity of rat resistance arteries ex-vivo. Activation of 5'AMP-activated protein kinase (AMPK) uncovers insulin-induced vasodilation in isolated muscle resistance arteries by stimulating NO and inhibiting ET-1 activity. A. the AMPK agonists globular adiponectin (gAdn) and 5-aminoimidazole-4-carboxamide-1-β-d-ribofuranoside (AICAR) uncover insulin-induced vasodilation in muscle resistance arteries. Depicted are vasoactive effects of insulin alone (white circles, n=5) and after pre-treatment with gAdn (white squares, n=6) (gAdn, 1 µg/mL) or AICAR (white triangles, n=5) (AICAR, 2 mmol/L). Responses are given as percent change from baseline diameter (see Methods). * $p<0.05$, ** $p<0.01$ gAdn + insulin vs. Insulin, # $p<0.05$ AICAR + insulin vs insulin. B. Effects of insulin plus gAdn or AICAR on the diameter of muscle resistance arteries during inhibition of ET-1. Vasoactive effects of insulin during inhibition of ET-1 (black circles, n=4) (PD142893, 3 µmol/L), and during inhibition of ET-1 after pre-treatment with gAdn (black squares, n=4) (gAdn, 1 µg/mL) or AICAR (black triangles, n=5) (AICAR, 2 mmol/L). * $p<0.05$ insulin + PD +gAdn vs. Insulin + PD + AICAR or Insulin + PD. C. gAdn inhibits vasoconstrictor effects of insulin during inhibition of NO synthesis. Vasoactive effects of insulin during inhibition of NO (harlequin circles, n=6) (LNA, 0.1mM), and during inhibition of NO after pre-treatment with gAdn (harlequin squares, n=6) (gAdn, 1.0 µg/mL) or AICAR (harlequin triangles n=5) (AICAR, 2 mmol/L). # $p<0.05$, ## $p<0.01$ gAdn plus LNA plus insulin vs. LNA plus insulin. * $p<0.05$, ** $p<0.01$ AICAR plus LNA plus insulin vs. LNA plus insulin.

figure 2 continued

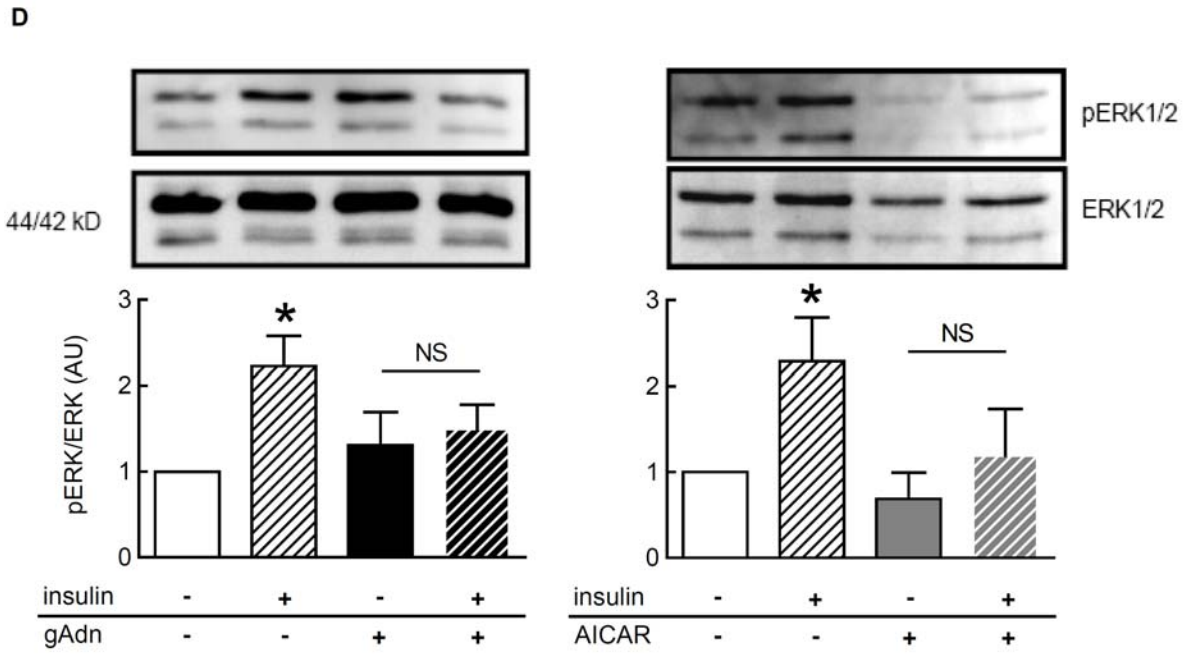

D. Inhibition of insulin-induced ERK phosphorylation by gAdn (black bars) and AICAR (grey bars) in rat resistance arteries. * $p<0.05$ vs. control (-/-).

figure 3

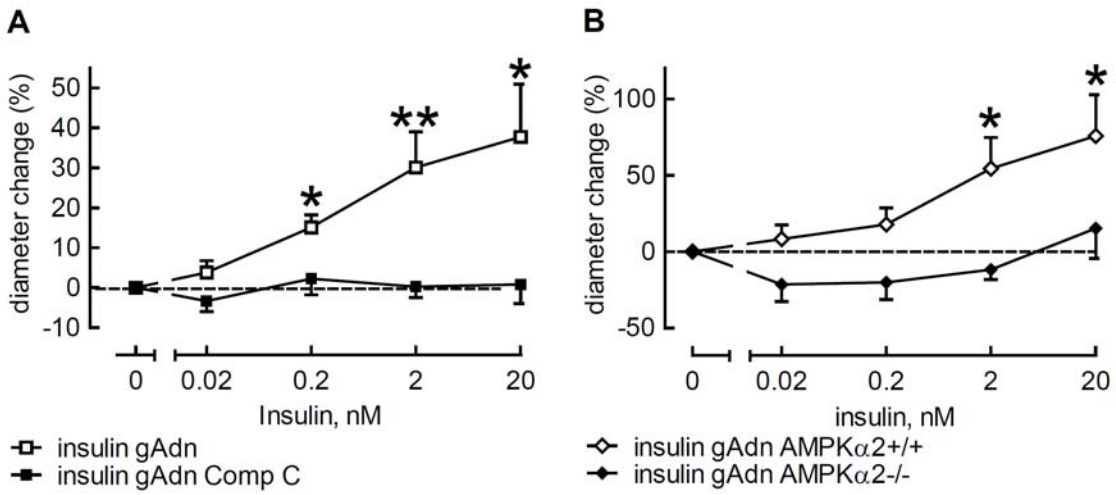

Interaction between globular adiponectin (gAdn) and insulin in muscle resistance arteries is mediated by 5'AMP-activated protein kinase α2 (AMPKα2). A. The AMPK inhibitor compound C abolishes insulin-induced vasodilation after pretreatment with gAdn in rat resistance arteries. Vasoactive effects of insulin after pre-treatment with gAdn (also shown in figure 2A, here for comparison with figure 2B, white squares, n=6) (gAdn, 1 μg/mL) and additional pretreatment with Compound C (black squares, n=5) (Compound C, 10 μmol/L). Responses are given as percent change from the baseline diameter. * $p<0.05$, ** $p<0.01$ gAdn plus Compound C plus insulin vs. gAdn plus insulin. B. Deletion of AMPKα2 in mice abolishes the insulin-induced vasodilation after pretreatment with gAdn (AMPKα2+/+ white diamonds, n=6 and AMPKα2-/- black diamonds, n=5). * $p<0.05$ AMPKα2+/+ vs. AMPKα2-/-.

figure 4

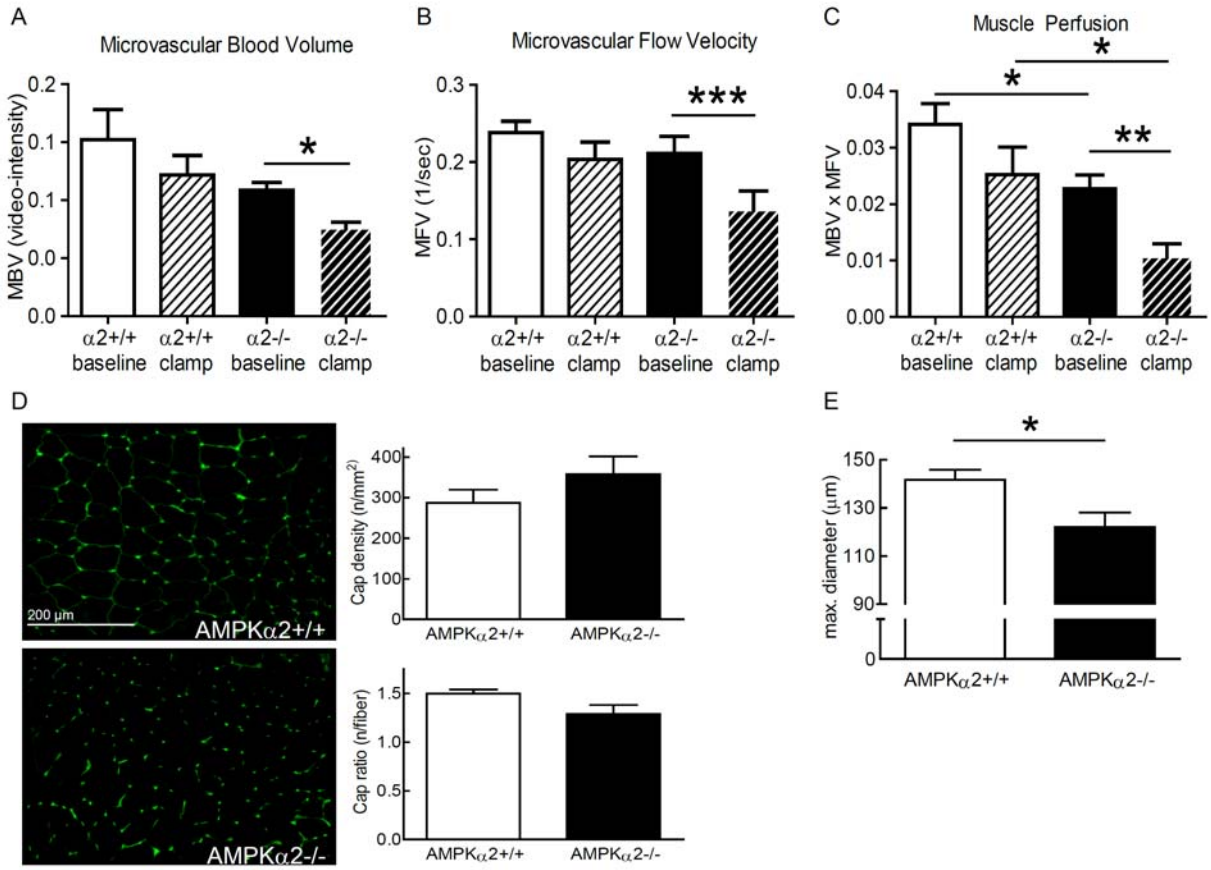

5'AMP-activated protein kinase α2 (AMPKα2) deletion impairs muscle perfusion and insulin sensitivity in vivo.
A. Microvascular blood volume (MBV) measured as video-intensity, decreased during the hyperinsulinemic clamp in AMPKα2-/- mice (n=5) by approximately 25% (*p<0.05, compared to baseline). B. Microvascular flow velocity (MFV) decreased during the hyperinsulinemic clamp in AMPKα2-/- mice (*p<0.0001, compared to baseline).
C. Skeletal muscle perfusion (MBVxMFV) was lower in AMPKα2-/- compared to AMPKα2+/+ (n=7) at baseline (*p<0.05). Skeletal muscle perfusion was decreased during the hyperinsulinemic clamp in AMPKα2-/- mice (**p<0.01). D. Skeletal muscle capillary density in AMPKα2-/- (n=3) and AMPKα2+/+ mice (n=4). Muscle capillaries were stain using lectin (see Methods). E. Maximal diameter of muscle resistance arteries in AMPKα2-/- (n=7) and AMPKα2+/+ mice (n=8), during incubation with the vasodilator papaverine (see Methods, *p<0.05).

figure 5

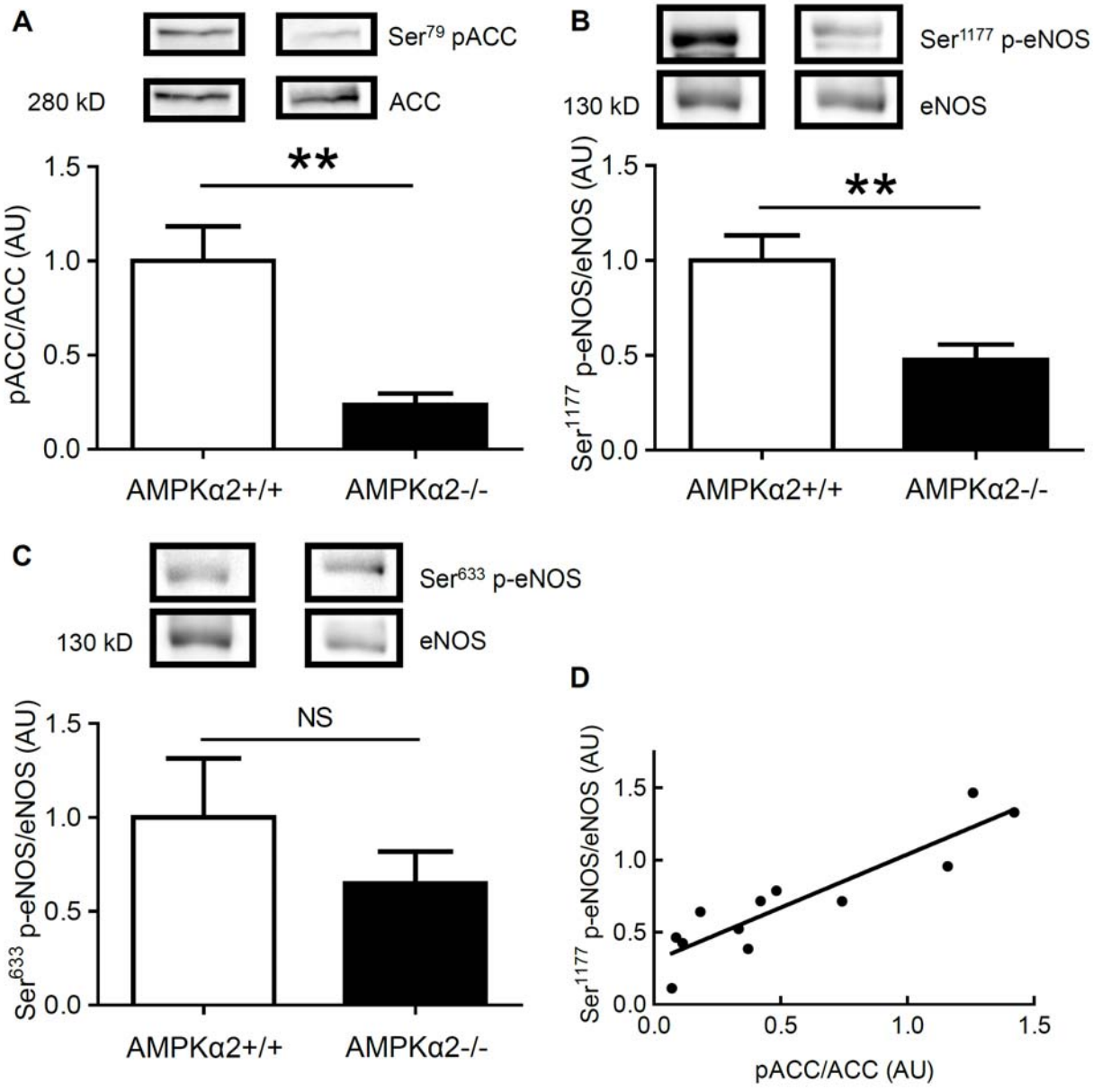

5'AMP-activated protein kinase α2 (AMPKα2) deletion strongly reduces vascular AMPK activity and eNOS phosphorylation in vivo. **A**: Deletion of AMPKα2 (n=7) impairs the phosphorylation of acetyl CoA carboxylase (ACC) in mouse skeletal muscle resistance arteries (**p<0.01 compared to AMPKα2 +/+ mice, n=5). **B**: Phosphorylation of eNOS at Ser^{1177} is impaired in AMPKα2 -/- (n=7) (**p<0.01 compared to AMPKα2 +/+ mice, n=6). **C**: Phosphorylation of eNOS at Ser^{633} does not differ between AMPKα2-/- (n=7) and AMPKα2+/+ mice (n=6). **D**: relationship between phosphorylated ACC levels and eNOS phosphorylation at Ser^{1177} (n=12, r^2=0.83, p<0.0001).

figure 6

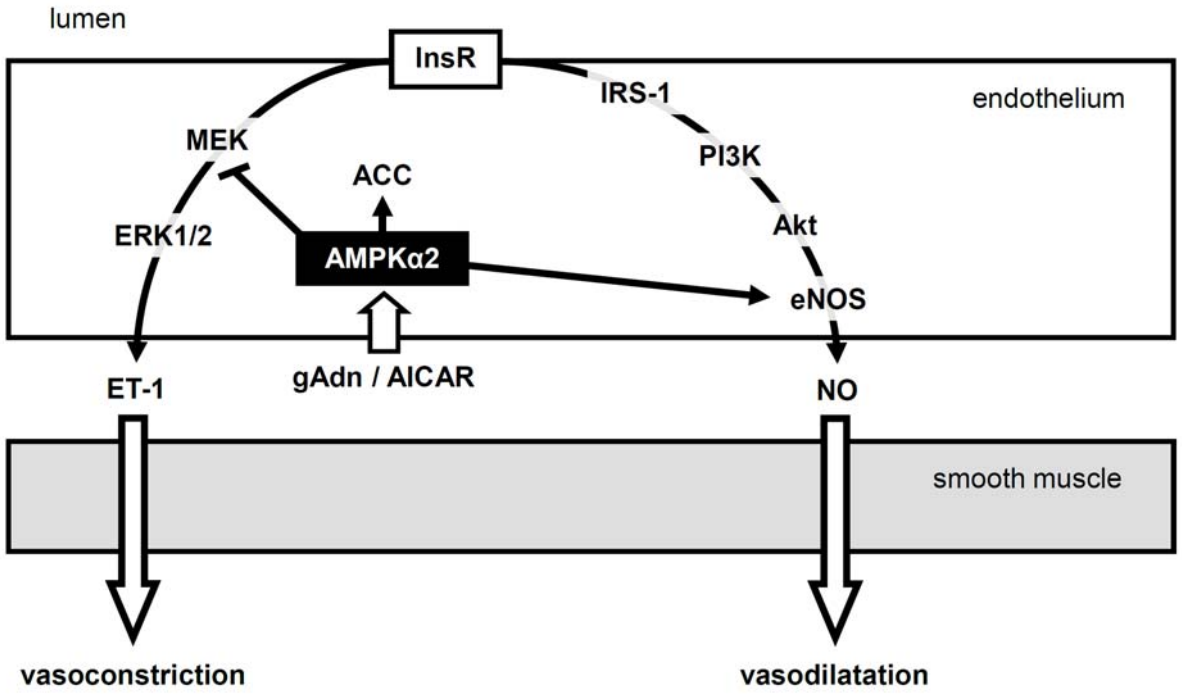

Schematic overview of the effects of globular adiponectin (gAdn) and 5-aminoimidazole-4-carboxamide-1-β-d-ribofuranoside (AICAR) on insulin signaling in muscle resistance arteries. gAdn and AICAR activate 5'AMP-activated protein kinase α2 (AMPKα2), inhibiting the MEK/ERK-1/2 signaling cascade and stimulation eNOS activity and subsequent NO production. This shifts the balance of insulin induced vasoreactivity to vasodilation. InsR=insulin receptor, MEK= mitogen-activated protein kinase, ERK1/2= extracellular signal-regulated kinase 1/2, IRS-1=insulin receptor substrate 1, PI3K=phosphatidylinositol 3-kinase, eNOS=endothelial nitric oxide synthase. ACC= acetyl CoA carboxylase, a downstream substrate of activated AMPK.

References

1 Sullivan PW, Morrato EH, Ghushchyan V, Wyatt HR, Hill JO. Obesity, inactivity, and the prevalence of diabetes and diabetes-related cardiovascular comorbidities in the U.S., 2000-2002. Diabetes Care 28: 1599-1603, 2005.

2 Viollet B, Andreelli F, Jørgensen SB et al. The AMP-activated protein kinase alpha2 catalytic subunit controls whole-body insulin sensitivity. J Clin Invest. 111: 91-98, 2003.

3 Zou MH, Hou XY, Shi CM, Nagata D, Walsh K, Cohen RA. Modulation by peroxynitrite of Akt- and AMP-activated kinase-dependent Ser1179 phosphorylation of endothelial nitric oxide synthase. J Biol Chem. 277: 32552-32557, 2002.

4 Hardie DG. AMPK: A Target for Drugs and Natural Products With Effects on Both Diabetes and Cancer. Diabetes 62: 2164-2172, 2013.

5 Ouyang J, Parakhia RA, Ochs RS. Metformin activates AMP kinase through inhibition of AMP deaminase. J Biol Chem. 286:1-11, 2011.

6 Frøsig C, Jensen TE, Jeppesen J, Pehmøller C, Treebak JT, Maarbjerg SJ, Kristensen JM, Sylow L, Alsted TJ, Schjerling P, Kiens B, Wojtaszewski JF, Richter EA. AMPK and insulin action-responses to ageing and high fat diet. PLoS One 8:e62338, 2013.

7 Kubota T, Kubota N, Kumagai H et al. Impaired insulin signaling in endothelial cells reduces insulin-induced glucose uptake by skeletal muscle. Cell Metab. 13: 294-307, 2011.

8 Barrett EJ, Wang H, Upchurch CT, Liu Z. Insulin regulates its own delivery to skeletal muscle by feed-forward actions on the vasculature. Am J Physiol Endocrinol Metab. 301: E252-263, 2011.

9 De Boer MP, Meijer RI, Wijnstok NJ, Jonk AM, Houben AJ, Stehouwer CD, Smulders YM, Eringa EC, Serné EH. Microvascular dysfunction: a potential mechanism in the pathogenesis of obesity-associated insulin resistance and hypertension. Microcirculation 19: 5-18, 2012.

10 Barrett EJ, Eggleston EM, Inyard AC, Wang H, Li G, Chai W, Liu Z. The vascular actions of insulin control its delivery to muscle and regulate the rate-limiting step in skeletal muscle insulin action. Diabetologia 52: 752-764, 2009.

11 Clerk LH, Vincent MA, Jahn LA, Liu Z, Lindner JR, Barrett EJ. Obesity blunts insulin-mediated microvascular recruitment in human forearm muscle. Diabetes 55: 1436-1442, 2006.

12 Eringa EC, Stehouwer CD, Merlijn T, Westerhof N, Sipkema P. Physiological concentrations of insulin induce endothelin-mediated vasoconstriction during inhibition of NOS or PI3-kinase in skeletal muscle arterioles. Cardiovasc Res. 56: 464-471, 2002.

13 Rattigan S, Clark MG, Barrett EJ. Hemodynamic actions of insulin in rat skeletal muscle: evidence for capillary recruitment. Diabetes 46: 1381-1388, 1997.

14 Eringa EC, Stehouwer CD, van Nieuw Amerongen GP, Ouwehand L, Westerhof N, Sipkema P. Vasoconstrictor effects of insulin in skeletal muscle arterioles are mediated by ERK1/2 activation in endothelium. Am J Physiol Heart Circ Physiol. 287: H2043-2048, 2004.

15 Eringa EC, Stehouwer CD, Walburg K, Clark AD, van Nieuw Amerongen GP, Westerhof N, Sipkema P. Physiological concentrations of insulin induce endothelin-dependent vasoconstriction of skeletal muscle resistance arteries in the presence of tumor necrosis factor-alpha dependence on c-Jun N-terminal kinase. Arterioscler Thromb Vasc Biol. 26: 274-280, 2006.

16 Zhao L, Chai W, Fu Z, Dong Z, Aylor KW, Barrett EJ, Cao W, Liu Z. Globular adiponectin enhances muscle insulin action via microvascular recruitment and increased insulin delivery. Circ Res. 112: 1263-1271, 2013.

17 Høeg LD, Sjøberg KA, Lundsgaard AM, Jordy AB, Hiscock N, Wojtaszewski JF, Richter EA, Kiens B. Adiponectin concentration is associated with muscle insulin sensitivity, AMPK phosphorylation, and ceramide content in skeletal muscles of men but not women. J Appl Physiol. 114: 592-601, 2013.

18 Hattori,Y, Suzuki,M, Hattori,S, Kasai,K. Globular adiponectin upregulates nitric oxide production in vascular endothelial cells. Diabetologia 46: 1543-1549, 2003.

19 Bradley,EA, Eringa,EC, Stehouwer,CDA, Korstjens,I, Nieuw Amerongen,GP, Musters,R, Sipkema,P, Clark,MG, Rattigan,S: Activation of AMP-Activated Protein Kinase by 5-Aminoimidazole-4-Carboxamide-1-beta-D-Ribofuranoside in the Muscle Microcirculation Increases Nitric Oxide Synthesis and Microvascular Perfusion. Arterioscler Thromb Vasc Biol 30: 1137-1142, 2010.

20 Aman J, van Bezu J, Damanafshan A, Huveneers S, Eringa EC, Vogel SM, Groeneveld AB, Vonk Noordegraaf A, van Hinsbergh VW, van Nieuw Amerongen GP. Effective treatment of edema and endothelial barrier dysfunction with imatinib. Circulation 126: 2728-2738, 2012.

21 Klibanov,AL, Rasche,PT, Hughes,MS, Wojdyla,JK, Galen,KP, Wible,JH, Jr., Brandenburger,GH. Detection of individual microbubbles of ultrasound contrast agents: imaging of free-floating and targeted bubbles. Invest Radiol 39: 187-195, 2004.

22 Wei,K, Jayaweera,AR, Firoozan,S, Linka,A, Skyba,DM, Kaul,S. Quantification of myocardial blood flow with ultrasound-induced destruction of microbubbles administered as a constant venous infusion. Circulation 97: 473-483, 1998.

23 Voshol PJ, Jong MC, Dahlmans VE, Kratky D, Levak-Frank S, Zechner R, Romijn JA, Havekes LM. In muscle-specific lipoprotein lipase-overexpressing mice, muscle triglyceride content is increased without inhibition of insulin-stimulated whole-body and muscle-specific glucose uptake. Diabetes 50: 2585-2590, 2001.

24 Potenza MA, Marasciulo FL, Chieppa DM, Brigiani GS, Formoso G, Quon MJ, Montagnani M. Insulin resistance in spontaneously hypertensive rats is associated with endothelial dysfunction characterized by imbalance between NO and ET-1 production. Am J Physiol Heart Circ Physiol. 289: H813-822, 2005.

25 Chen Z, Peng IC, Sun W, Su MI, Hsu PH, Fu Y, Zhu Y, DeFea K, Pan S, Tsai MD, Shyy JY. AMP-activated protein kinase functionally phosphorylates endothelial nitric oxide synthase Ser633. Circ Res. 104: 496-505, 2009.

26 Xu MJ, Song P, Shirwany N, Liang B, Xing J, Viollet B, Wang X, Zhu Y, Zou MH. Impaired expression of uncoupling protein 2 causes defective postischemic angiogenesis in mice deficient in AMP-activated protein kinase α subunits. Arterioscler Thromb Vasc Biol. 31: 1757-1765, 2011.

27 Schisler JC, Rubel CE, Zhang C, Lockyer P, Cyr DM, Patterson C. CHIP protects against cardiac pressure overload through regulation of AMPK. J Clin Invest. 123: 3588-3599, 2013.

28 Scott JW, Ling N, Issa SM, Dite TA, O'Brien MT, Chen ZP, Galic S, Langendorf CG, Steinberg GR, Kemp BE, Oakhill JS. Small molecule drug A-769662 and AMP synergistically activate naive AMPK independent of upstream kinase signaling. Chem Biol. 21: 619-627, 2014.

29 Bakker EN, Buus CL, VanBavel E, Mulvany MJ. Activation of resistance arteries with endothelin-1: from vasoconstriction to functional adaptation and remodeling. J Vasc Res. 41: 174-182, 2004.

30 Zwetsloot KA, Westerkamp LM, Holmes BF, Gavin TP. AMPK regulates basal skeletal muscle capillarization and VEGF expression, but is not necessary for the angiogenic response to exercise. J Physiol. 586: 6021-6035, 2008.

31 Morrow VA, Foufelle F, Connell JM, Petrie JR, Gould GW, Salt IP. Direct activation of AMP-activated protein kinase stimulates nitric-oxide synthesis in human aortic endothelial cells. J Biol Chem. 278: 31629-31639, 2003.

32 Meijer RI, Bakker W, Alta CL, Sipkema P, Yudkin JS, Viollet B, Richter EA, Smulders YM, van Hinsbergh VW, Serné EH, Eringa EC. Perivascular Adipose Tissue Control of Insulin-Induced Vasoreactivity in Muscle Is Impaired in db/db Mice. Diabetes 62: 590-598, 2013.

33 Yudkin JS, Eringa E, Stehouwer CD. "Vasocrine" signalling from perivascular fat: a mechanism linking insulin resistance to vascular disease. Lancet. 365: 1817-1820, 2005.

34 Mu J, Brozinick JT Jr, Valladares O, Bucan M, Birnbaum MJ. A role for AMP-activated protein kinase in contraction- and hypoxia-regulated glucose transport in skeletal muscle. Mol Cell. 7: 1085-1094, 2001.

35 Meijer RI, De Boer MP, Groen MR, Eringa EC, Rattigan S, Barrett EJ, Smulders YM, Serne EH. Insulin-induced microvascular recruitment in skin and muscle are related and both are associated with whole-body glucose uptake. Microcirculation 19: 494-500, 2012.

36 Vincent MA, Barrett EJ, Lindner JR, Clark MG, Rattigan S. Inhibiting NOS blocks microvascular recruitment and blunts muscle glucose uptake in response to insulin. Am J Physiol Endocrinol Metab. 285: E123-129, 2003.

37 Shemyakin A, Salehzadeh F, Böhm F, Al-Khalili L, Gonon A, Wagner H, Efendic S, Krook A, Pernow J. Regulation of glucose uptake by endothelin-1 in human skeletal muscle in vivo and in vitro. J Clin Endocrinol Metab. 95: 2359-2366, 2010.

38 Chalothorn D, Faber JE. Strain-dependent variation in collateral circulatory function in mouse hindlimb. Physiol Genomics. 42: 469-479, 2010.

Supplemental material

figure 1

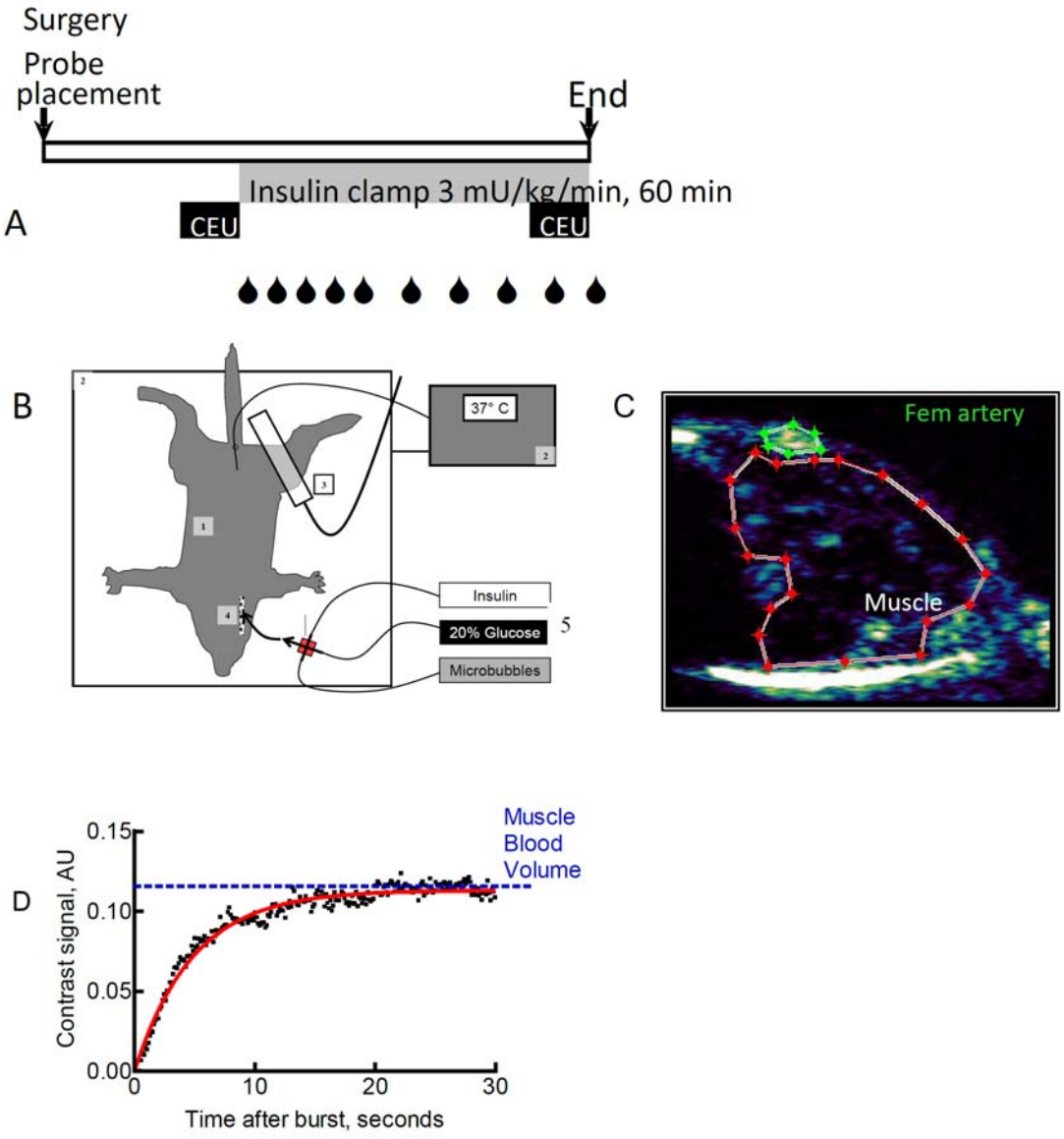

A. Time course of the hyperinsulinemic euglycemic clamp. CEU indicates contrast enhanced ultrasound. Drop indicates blood sampling. B. Schematic representation of experimental setup. 1 mouse. 2 homeothermic heating pad. 3 ultrasound probe. 4 infusion of jugular vein. 5 perfusor pumps. C. CEU. Cross-section proximal adductor muscle group hindleg. Regions of interest showing femoral artery and skeletal muscle. D. CEU replenishment curve. AU indicates arbitrary units.

figure 2

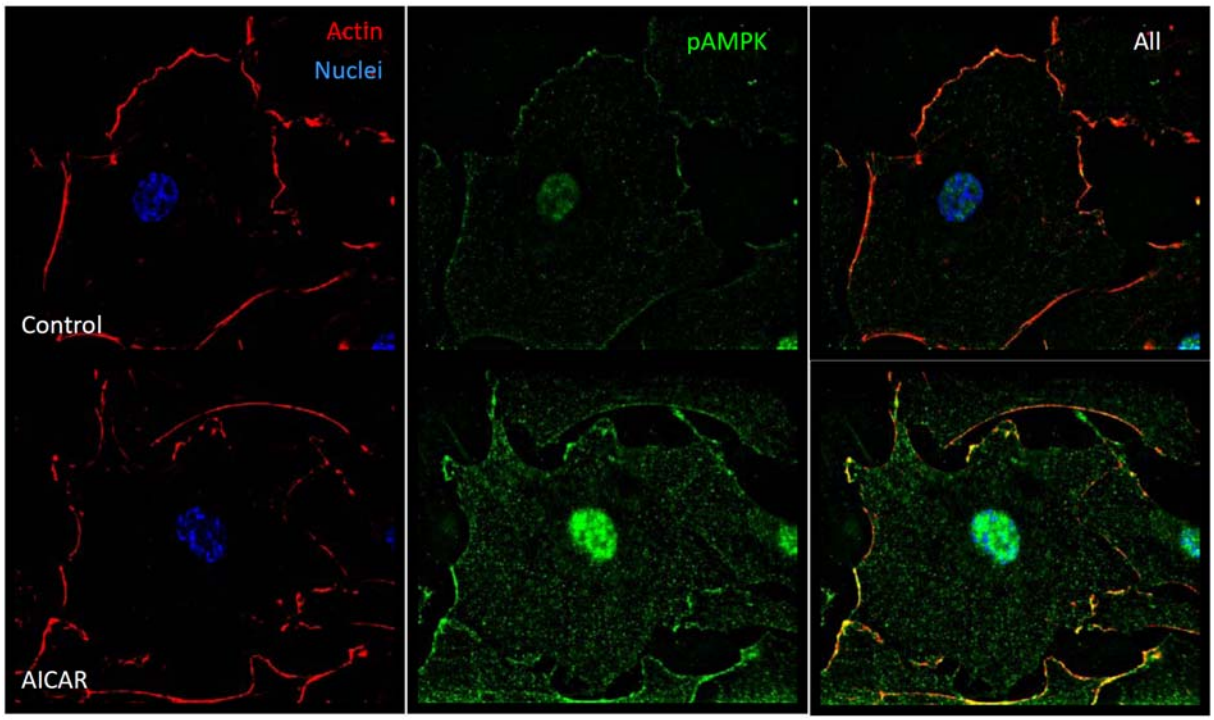

Activation of AMPK by AICAR and its localization in human microvascular endothelial cells. Localization of pAMPKα in human microvascular endothelial cells using three-dimensional deconvolution microscopy at 63x magnification.

figure 3

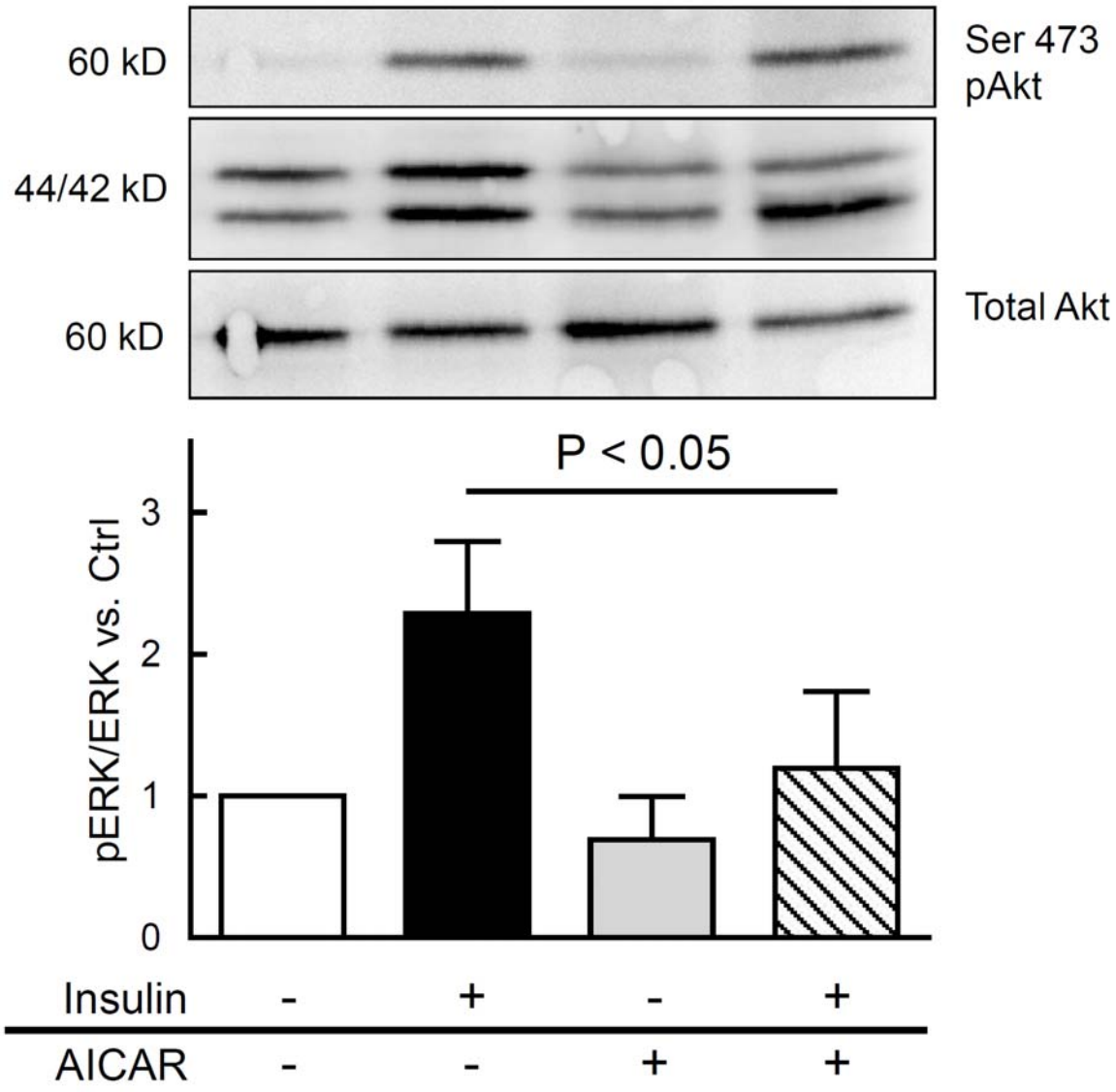

AMPK activation by AICAR does not enhance insulin-induced Ser473 phosphorylation of Akt in muscle resistance arteries. Insulin preincubation 2nmol/L.

figure 4

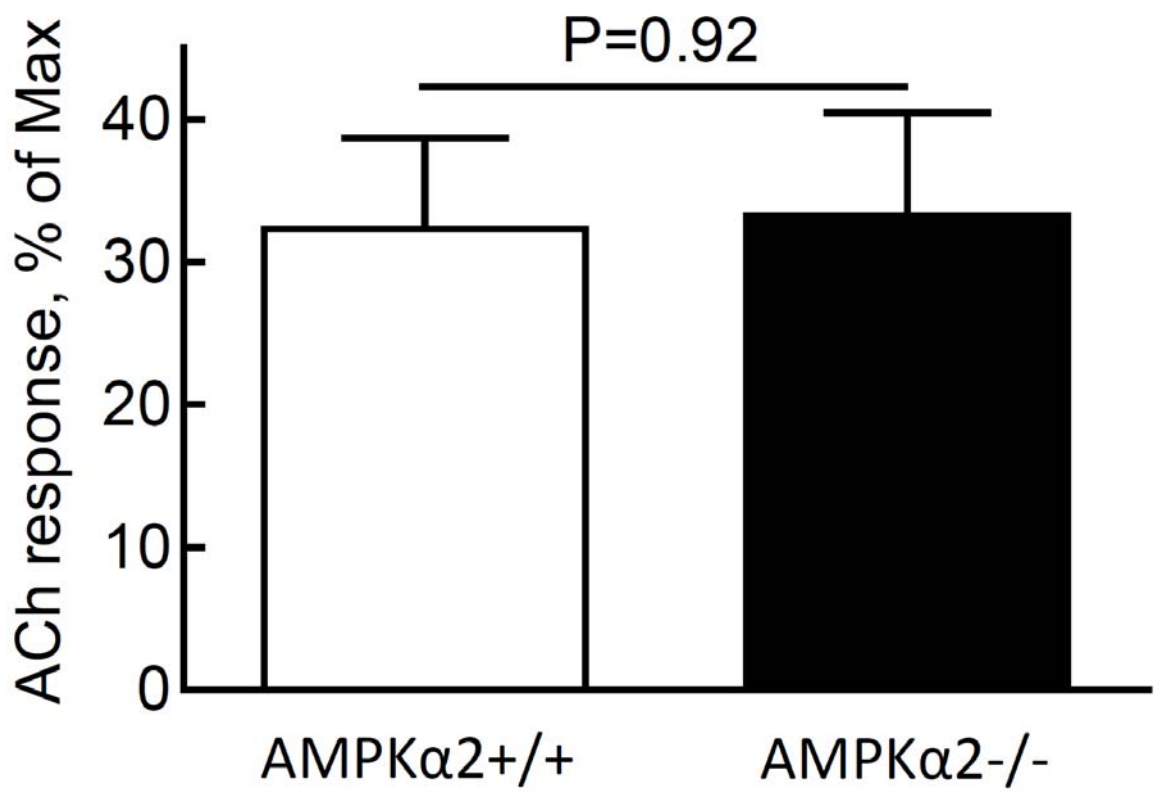

The effect of genetic deletion of AMPKα2 on general endothelium-dependent vasodilation. ACh indicates the endothelium-dependent vasodilator acetylcholine (0.1 μmol/L; Sigma, St Louis, USA). Max indicates maximal luminal diameter in pressure myograph.

figure 5

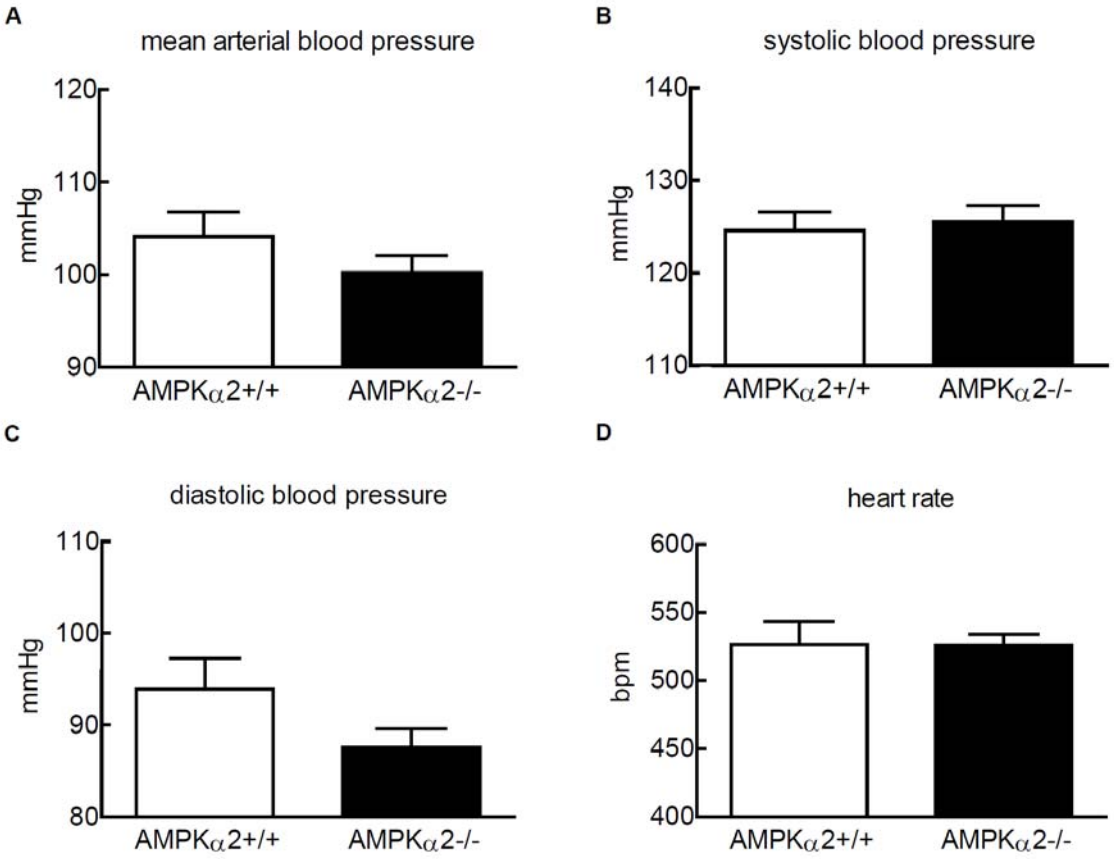

Systemic arterial blood pressure and heart rate did not differ between the 5'AMP-activated protein kinase α2 (AMPKα2) -/- and AMPKα2+/+ mice. Average measurements during 48hrs of telemetry (see methods). A. Mean arterial blood pressure. B. Systolic blood pressure. C. Diastolic blood pressure. D. Heart rate.